AFRL-SN-HS-TR-2005-036

WIDEBAND CONFORMAL ANTENNAS AND ARRAYS

Jennifer T. Bernhard
Joshua A. Fladie

University of Illinois at Urbana-Champaign
1406 West Green Street
Urbana, Illinois

15 December 2005

Final Report

AIR FORCE RESEARCH LABORATORY
Sensors Directorate
Electromagnetics Technology Division
80 Scott Drive
Hanscom AFB MA 01731-2909

TECHNICAL REPORT

Title: Wideband Conformal Antennas and Arrays
Contract Number: FA8718-04-C-0060
Contractor: University of Illinois at Urbana-Champaign

Unlimited, Statement A

NOTICE

USING GOVERNMENT DRAWINGS, SPECIFICATIONS, OR OTHER DATA INCLUDED IN THIS DOCUMENT FOR ANY PURPOSE OTHER THAN GOVERNMENT PROCUREMENT DOES NOT IN ANY WAY OBLIGATE THE US GOVERNMENT. THE FACT THAT THE GOVERNMENT FORMULATED OR SUPPLIED THE DRAWINGS, SPECIFICATIONS, OR OTHER DATA DOES NOT LICENSE THE HOLDER OR ANY OTHER PERSON OR CORPORATION; OR CONVEY ANY RIGHTS OR PERMISSION TO MANUFACTURE, USE, OR SELL ANY PATENTED INVENTION THAT MAY RELATE TO THEM.

THIS TECHNICAL REPORT HAS BEEN REVIEWED AND IS APPROVED FOR PUBLICATION.

_____//signature//_____
BRADLEY C. KAANTA, 2nd LT, USAF
Contract Monitor
Antenna Technology Branch
Electromagnetics Technology Division

_____//signature//_____
LIVIO D. POLES
Chief, Antenna Technology Branch
Antenna Technology Branch
Electromagnetics Technology Division

_____//signature//_____
MICHAEL N. ALEXANDER
Technical Advisor
Electromagnetics Technology Division

REPORT DOCUMENTATION PAGE

Form Approved
OMB No. 0704-0188

1. REPORT DATE *(DD-MM-YYYY)*	2. REPORT TYPE	3. DATES COVERED *(From - To)*
17-10-2005	Final Report	August 2004 – July 2005

4. TITLE AND SUBTITLE
Wideband Conformal Antennas and Arrays

5a. CONTRACT NUMBER
FA8718-04-C-0060

5b. GRANT NUMBER

5c. PROGRAM ELEMENT NUMBER
62204F

6. AUTHOR(S)

Jennifer T. Bernhard
Joshua A. Fladie

5d. PROJECT NUMBER
4916

5e. TASK NUMBER
HA

5f. WORK UNIT NUMBER
05

7. PERFORMING ORGANIZATION NAME(S) AND ADDRESS(ES)

University of Illinois at Urbana-Champaign
1406 West Green Street
Urbana, Ilinois 61801

8. PERFORMING ORGANIZATION REPORT NUMBER

9. SPONSORING / MONITORING AGENCY NAME(S) AND ADDRESS(ES)

Electromagnetics Technology Division
Sensors Directorate
Air Force Research Laboratory/SNHA
80 Scott Drive
Hanscom AFB, MA 01731-2909

10. SPONSOR/MONITOR'S ACRONYM(S)
AFRL/SNHA

11. SPONSOR/MONITOR'S REPORT NUMBER(S)
AFRL-SN-HS-TR-2005-036

12. DISTRIBUTION / AVAILABILITY STATEMENT
Approved for public release; distribution unlimited

13. SUPPLEMENTARY NOTES

14. ABSTRACT

Report developed under contract FA8718-04-C-0060. The work done investigates some unexplored degrees of freedom in microstrip antenna design with the goal of developing a modified substrate configuration with improved bandwidth and maintained radiation characteristics. Results indicate that sectioned substrates can deliver increased impedance bandwidth. A closed-form circuit-based model is also developed to predict the performance of these new antenna structures. The modified substrate techniques developed here will be used along with loading and slot etching techniques studied previously to construct wideband planar antennas and arrays.

15. SUBJECT TERMS
wideband antennas; wideband arrays; sectioned substrates

16. SECURITY CLASSIFICATION OF:			17. LIMITATION OF ABSTRACT	18. NUMBER OF PAGES	19a. NAME OF RESPONSIBLE PERSON
a. REPORT	b. ABSTRACT	c. THIS PAGE			Bradley Kaanta
Unclassified	Unclassified	Unclassified	SAR	22	19b. TELEPHONE NUMBER *(include area code)* 781-377-0659

Standard Form 298 (Rev. 8-98)
Prescribed by ANSI Std. 239.18

TABLE OF CONTENTS

LIST OF FIGURES

1.0 Project Summary

In this project, we are investigating two aspects of wideband planar array design and behavior: (1) the fundamental characterization of suitable wideband conformal microstrip-based antennas as single elements and in arrays and (2) an exploration of possible approaches to expand the operating frequency bands and performance of planar and conformal arrays. These approaches encompass the use of novel substrates and antenna designs, array designs that allow wideband performance, such as random and connected array topologies, and implementation of antenna reconfiguration to enable wideband operation of planar and conformal arrays. The investigation uses the facilities of the Electromagnetics Laboratory, including commercial simulation packages, a specialized fabrication facility, and an antenna test facility that includes state-of-the-art measurement equipment and an anechoic chamber. One graduate student, Mr. Joshua Fladie (US Citizen), worked on the project. His progress to date is summarized below. He will be continuing this work to complete his M.S. thesis in the Spring of 2006.

2.0 Technical Progress Report

2.1 Background/Introduction

Microstrip patch antenna (MPA) designs are ideal for military applications because they are low profile, durable, inexpensive, and functionally robust. These same designs however, are characteristically narrowband. Techniques for increasing these narrowband designs have been developed, the most thoroughly investigated of which are passive element loading techniques [1-3], active element loading techniques [4-6] and slot etching techniques [7-9]. Bandwidth improvements using these techniques are moderate, but further increases in bandwidth are desired. A technique that possesses the capability to fulfill this need that has yet to be thoroughly investigated is electrical parameter variation in the substrate region of the MPA designs. Work done by Kiziltas [10] makes use of such a technique. In her work, the substrate is discretized into a large number cubic elements with varying permittivity. Using an algorithm, the layout and permittivity perturbations of these cubic elements is optimized. Resulting designs realized with this approach give increased impedance bandwidths. However, in the optimization scheme used, there is no control or specification on the radiation patterns and as a result there are still many improvements to be made. Work done by Mosallaei [11] also makes use of a

technique utilizing substrate variations. In his work he utilizes an engineered magneto-dielectric material composed of a woodpile arrangement of electric and magnetic materials as the substrate. The effect of this material is to provide a given miniaturization factor while providing bandwidths the same as for a design with a much smaller factor, making use of reduced fringing field confinement. Bandwidth improvements using this technique are, at the present time, only marginal. However, a number of unexplored degrees of freedom exist that have not been considered. The work done here, through this grant, investigates a few of these unexplored degrees of freedom with the goal of developing a modified substrate configuration with improved bandwidth and maintained radiation characteristics. The final goal for this work will be to use the modified substrate techniques developed here along with loading and slot etching techniques studied previously.

2.2 Choice of Substrate Variations

A large number of options exist in the use of variations in the substrate region of the MPA designs. We narrow down these options by considering substrates with variations in permittivity only. To further reduce these options we make use of some MPA theory. We take in account the fact that the basic radiating mechanism for many MPA designs is the fringing field and that the material properties of the substrate in the vicinity of these fields play an important role. Low permittivity material makes these fields less confined while high permittivity material makes these fields more confined. This effect is evident when studying the bandwidths of MPA designs on low and high permittivity substrates, with greater bandwidths delivered for designs on lower permittivity substrates. We studied permittivity variations in the substrate in the regions surrounding the radiating fringing fields. In our investigation we used a linearly polarized rectangular patch antenna and investigated a substrate that is sectioned into three block-like regions: two that are on the outer regions of the substrate, near the radiating edges, and one that is on inner region of the substrate. Figure 1 shows a three-dimensional depiction of this sectioned substrate geometry.

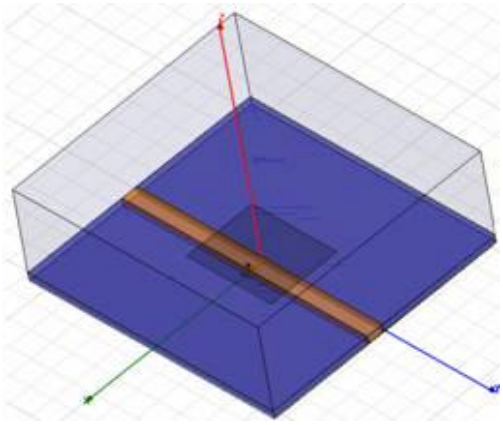

Figure 1. Three-dimensional view of the sectioned substrate geometry.

2.3 Simulation Studies

We investigated these sectioned substrate patch designs with the full wave simulator HFSS [12]. In doing so we first obtained results for a reference simple substrate design and then obtained results for a series of sectioned substrate designs. In order to make the comparisons of these different designs clear, we used identical patch dimensions, substrate height, and feed probe location. We also used sectioned substrate permittivity assignments to provide resulting center frequencies near the simple substrate center frequency by studying sectioned substrates in two configurations: one where the permittivities in the outer and inner regions were respectively, lower and higher than the simple substrate permittivity (LHL) and the other were there was an inverse arrangement (HLH). With these two configurations we studied the characteristics by completing simulations with increasing inner section size as is shown in Figure 2.

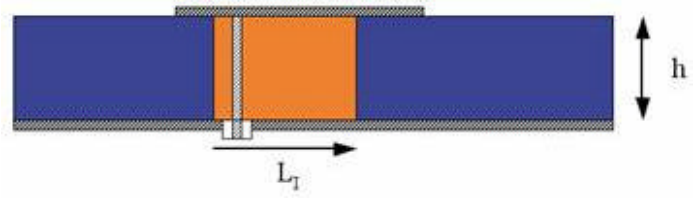

Figure 2. Side view of the sectioned substrate showing dimensions and length variations.

2.3A. Simple Substrate

A center frequency of 3 GHz and a relative permittivity of 2.2 were used as the design specifications for the simple substrate patch. Patch dimensions for these specifications were found to be a length of 3.08 cm and a width of 3.95 cm. The probe was located 8.9 mm from the radiating edge of the patch and centered along the patch width. The height of the patch above the ground plane was chosen to be 3.175 mm. Figures 2 and 3 show these dimensions.

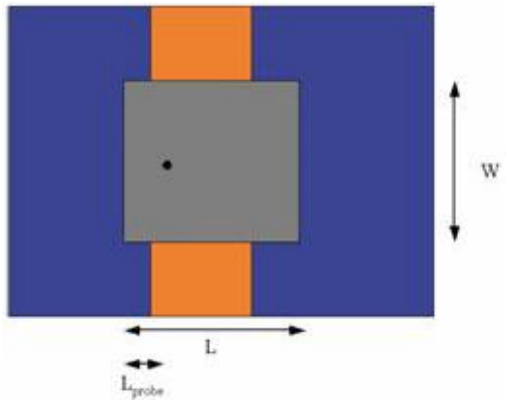

Figure 3. Top view of the sectioned substrate.

Modeling and simulation of this patch in HFSS resulted in the standard input and radiation characteristics shown in Figure 4. As is usual, the bandwidth of the antenna is narrow, giving a 4.0 percent bandwidth 2:1 VSWR bandwidth where percent bandwidth is defined in [13]. The impedances shown on the Smith chart are inductive and the radiation patterns at the center frequency are broadside with a very wide beam width.

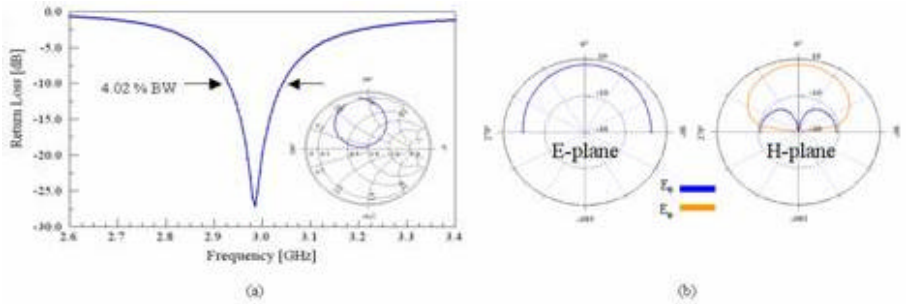

Figure 4. Simple substrate input characteristics (a) and radiation patterns (b).

2.3B. Sectioned Substrate (LHL)

Using the HFSS model for the simple substrate design, we divided the substrate into three sectioned substrate regions. We then assigned a permittivity value to each of these three regions following the LHL configuration definition. The values we used for these regions were offsets of 0.3 from the simple substrate value of 2.2.

With this model, we completed simulations for the inner section having a size of 7 mm, 12 mm, 17 mm, 22 mm, and 27 mm. The resulting return loss curves are shown in Figure 5a. The center frequencies for these curves decrease with frequency as the size of the inner, higher permittivity, section increases. Considering this sectioned substrate as a single substrate with an effective permittivity, this is an expected result. VSWR equal to 2 percentage bandwidths are shown in Figure 6 for the results found using this LHL configuration and also for the results found using the HLH configuration. The peak bandwidth result among these LHL configurations is 4.4%, a 10% improvement upon the simple substrate bandwidth. Impedance results are shown in the Smith chart in Figure 5a and the impedances maintain values close to the values found for the simple substrate design. Figure 5b shows the radiation pattern result for an inner section size of 22 mm at 3.03 GHz. This pattern is nearly identical to the simple substrate pattern, this pointing to the conclusion that the patterns are maintained for these sectioned substrate patches.

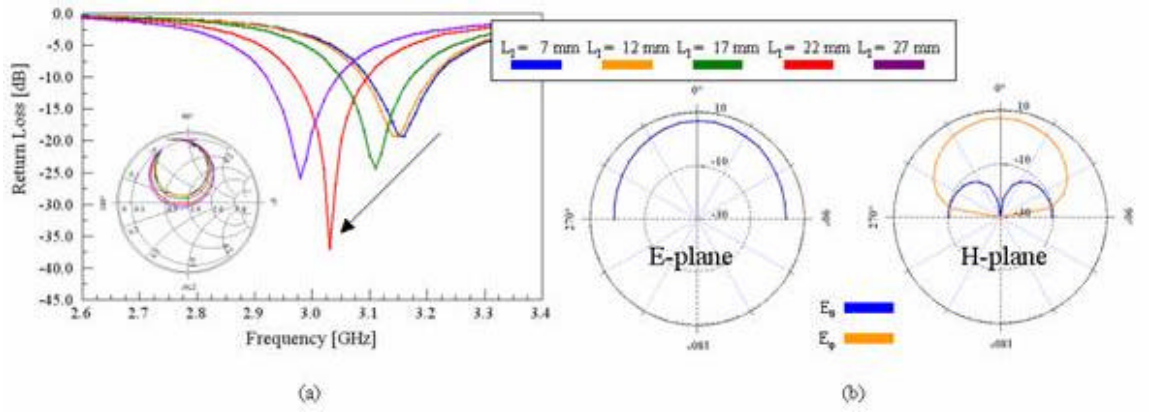

Figure 5. LHL configuration input characteristics (a) and radiation patterns (b).

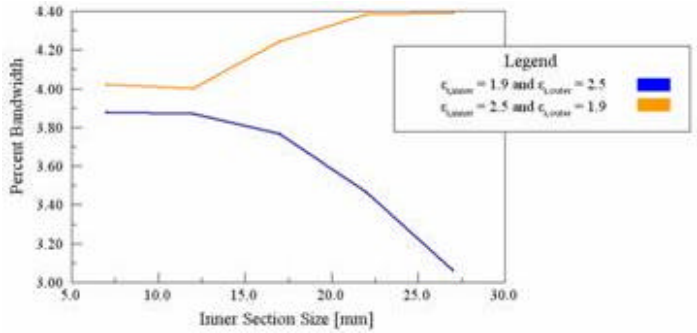

Figure 6. Percent bandwidth results for the LHL and HLH configurations.

2.3C. Sectioned Substrate (HLH)

We studied the HLH configuration in the same manner as the LHL configuration. Permittivity assignments were the same as for the LHL configuration but were inverted. The resulting return loss curves are shown in Figure 7a. Examining these curves, a similar but opposite trend emerges. With the increasing size of the inner, lower permittivity, section comes an increase in the center frequencies of the return loss curves. Again, this is an expected result considering this sectioned substrate as a single substrate with an effective permittivity. VSWR equal to 2 percentage bandwidths are provided for this configuration in Figure 6. The results ake an opposite trend to the bandwidth results seen in the LHL configurations with percentage bandwidths from 3.8% down to as low as 3.1%. Impedance results are shown along with the return loss results in Figure 7a and can again be seen to be close to the simple substrate results. Figure 7b shows the radiation pattern result for an inner section size of 12 mm at 2.84 GHz. Again this pattern is nearly identical to the simple substrate pattern.

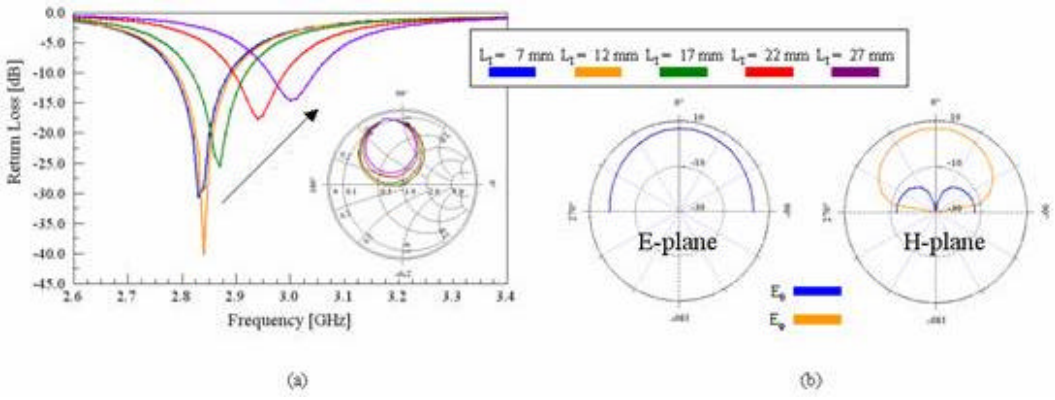

Figure 7. HLH configuration input characteristics (a) and radiation patterns (b).

2.4 Effective Permittivity Analysis

As a first analysis approach, we studied these sectioned substrates as effective mediums. In doing so, we used a quasi-static capacitance approach. This was applied to our sectioned substrate designs by considering them as parallel plate capacitors.

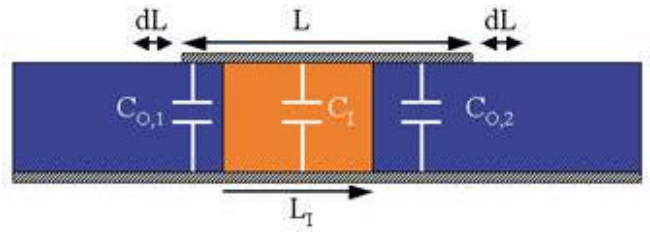

Figure 8. Side view of the sectioned substrate showing the effective capacitances.

Figure 8 shows a generic sectioned substrate from a side view and shows how the sectioned substrate patch can be broken down into three parallel capacitances $C_{O,1}$, $C_{O,2}$, and C_I. Using the basic expression for the capacitance of parallel plate capacitors,

$$C = \frac{\varepsilon LW}{h}, \tag{1}$$

along with the equivalent capacitance expression for parallel capacitors,

$$C_{eq} = C_1 + C_2 + C_3 + \ldots, \tag{2}$$

we were able to arrive at an effective permittivity expression. This expression was incomplete because it did not take the differential fringing field lengths into account. Adding the differential lengths, given by [14]

$$dL = 0.412\,h\frac{(\varepsilon_{eff}+0.3)(W/h+0.262)}{(\varepsilon_{eff}-0.258)(W/h+0.813)}, \tag{3}$$

where ε_{eff} is given by

$$\varepsilon_{eff} = \frac{\varepsilon_r+1}{2} + \frac{\varepsilon_r-1}{2\sqrt{1+10h/W}}, \tag{4}$$

into the expressions we obtained the final expression given by

$$\varepsilon_{eff,ss} = \left(\frac{L_I}{L+2dL}\right)\varepsilon_{r,inner} + \left(\frac{L_O}{L+2dL}\right)\varepsilon_{r,outer}, \quad (5)$$

where L_O is given by

$$L_O = (L + 2dL) - L_I. \quad (6)$$

With this expression we determined effective permittivity values for each of the previously studied sectioned substrates. We then ran simulations of the simple substrate patch with the substrate permittivity using each of the effective permittivity values. To study the resulting data we plotted the center frequencies versus inner section volume fraction where the inner section volume fraction was the ratio of L_I to L_O. Figure 9 gives this plot for the LHL and HLH configurations with data from both the effective permittivity HFSS results and the direct HFSS results.

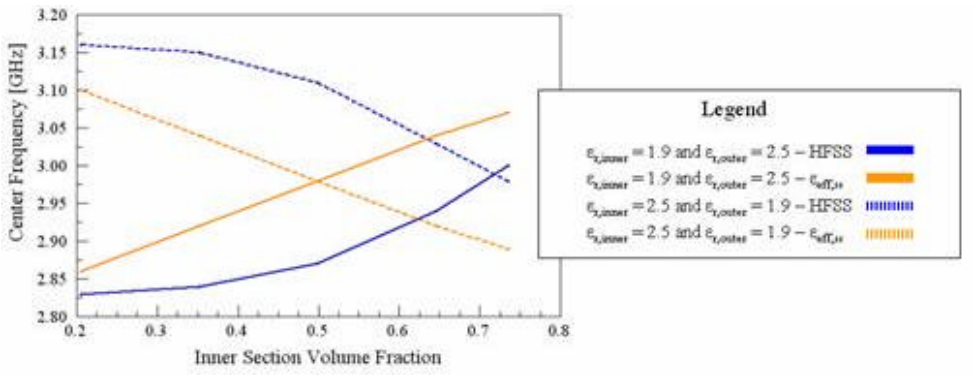

Figure 9. Center frequency results versus inner section volume fraction.

Looking at the curves for the LHL configurations, it can be seen that the values found using the effective permittivity approach consistently underestimate the direct HFSS results. Additionally, the curves for the HLH configurations found using the effective permittivity approach consistently overestimate the direct HFSS results. Considering the inverse relationship between

effective permittivity and center frequency, and considering the above trends, we observe that the center frequency values found using the effective permittivity approach would better match the more exact HFSS results if the value of the permittivity in the outer regions carried a greater weighting in the effective permittivity expression. For this quasi-static capacitance approach however, it seems that the modeling is a little unsatisfactory and from this we came to the realization that this approach is better suited for a more continuous medium.

2.5 Transmission Line Modeling

As an alternative to the effective permittivity analysis approach, we developed a transmission line (TL) model [15]. The model, for the simple substrate case, of two parallel TL branches with resistive loading at the end of each branch. The characteristic impedances of the lines were determined directly from the microstrip expression [16],

$$Z_c = \frac{120\pi}{\sqrt{\varepsilon_{eff}}\left[W/h + 1.393 + 0.667\ln(W/h + 1.444)\right]}. \qquad (7)$$

The loads were modeled using the conductance expression [17]

$$G = \frac{W}{120\lambda}\left[1 - \frac{\pi^2}{6}(h/\lambda)^2\right] \qquad (8)$$

and the fringing fields were modeled using Eq. (3). Modeling of the probe was completed using a PI network equivalent [18], shown in Figure 10, where the values of the elements were found by comparison with direct HFSS results. Adaptation of this overall TL model for the sectioned substrate designs was completed by simply breaking each of the TL branches into series sections of TL mimicking the sectioning of the substrate. Figure 11 shows this model for the three-section substrate patch antenna probe fed on the interior of the middle of the inner section.

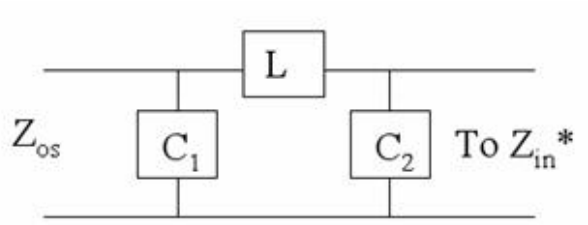

Figure 10. PI network equivalent for the probe model.

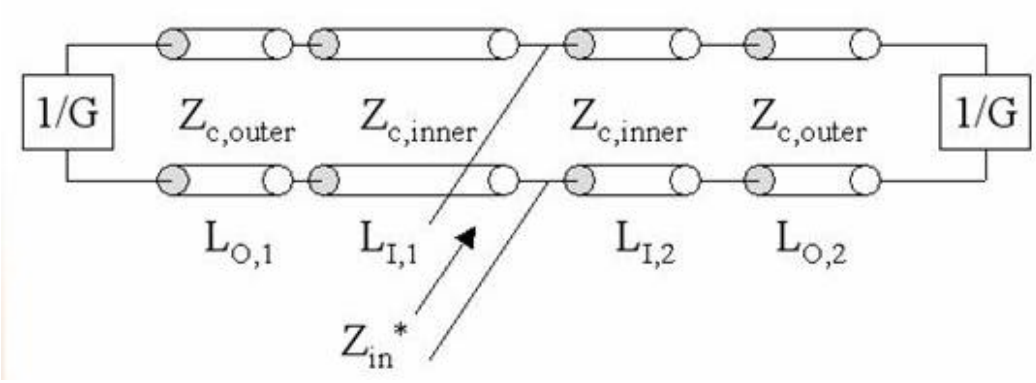

Figure 11. Sectioned substrate TL model diagram.

Using MATLAB, the TL model was implemented to give return loss and impedance results over frequency. The model results for the simple substrate design in comparison with the direct HFSS simulation results are given in Figure 12.

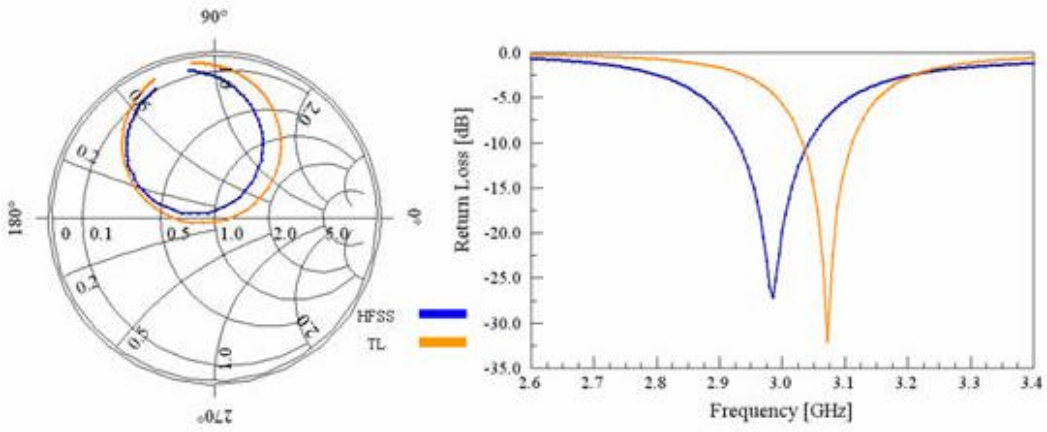

Figure 12. TL and HFSS results for the simple substrate design.

The impedance results for the TL model match the direct HFSS results quite well. Observing the return loss results, an approximately 100 MHz frequency shift can be seen between the center frequencies for the TL model and direct HFSS results with the TL model results being lower in frequency.

Utilizing the model for the previously studied sectioned substrate configurations we were able to obtain the return loss results shown in Figure 13. It is evident that the trends with the increasing size of the inner sections remain and that the TL model results follow direct HFSS results fairly well with the exception of a frequency shift of about 100 MHz.

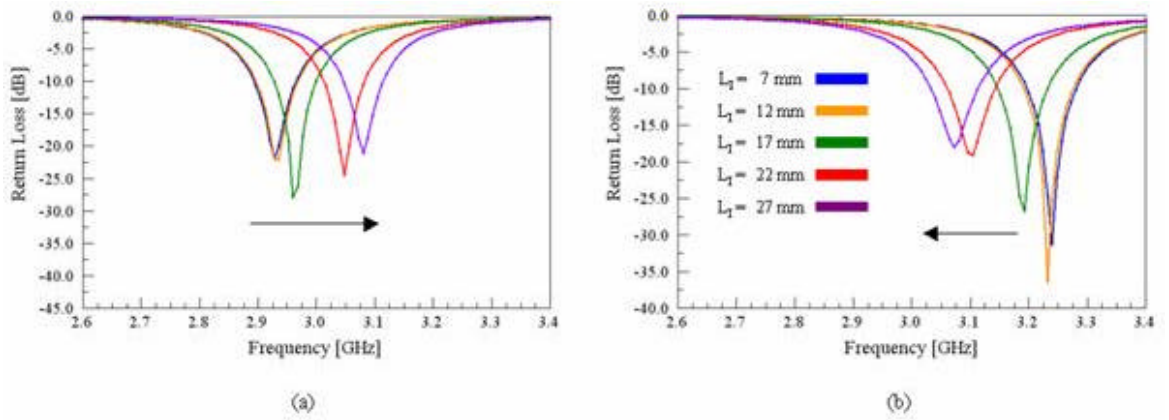

Figure 13. TL model results for the HLH configurations (a) and for the LHL configurations (b).

Plotting the center frequencies for these results versus inner section volume fraction as we did with the effective permittivity analysis, we see that the TL results match the direct HFSS results quite well with the exception of the 100 MHz frequency shift.

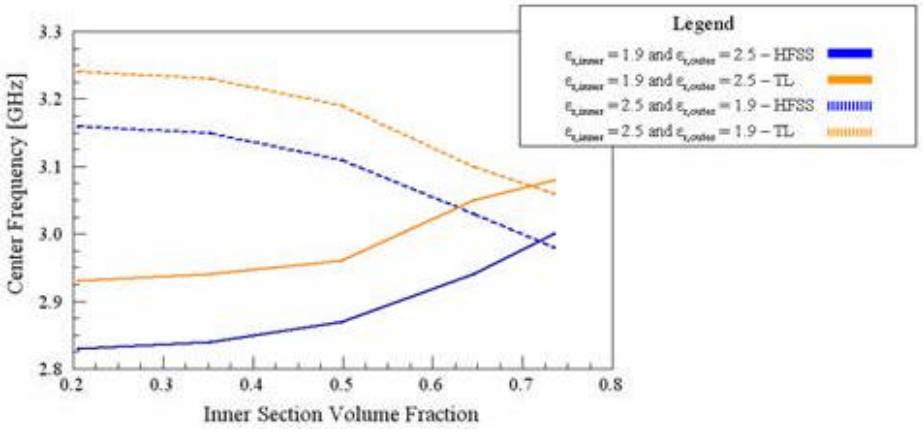

Figure 14. Center frequency versus inner section volume fraction plot for TL model results and direct HFSS results.

Considering our many past experiences with HFSS results overestimating measured results, we plotted the center frequencies versus the inner section volume fraction with a 100 MHz frequency shift removed from the direct HFSS results, Figure 14. As can be seen in the figure, the data points match up very well with this shift removed.

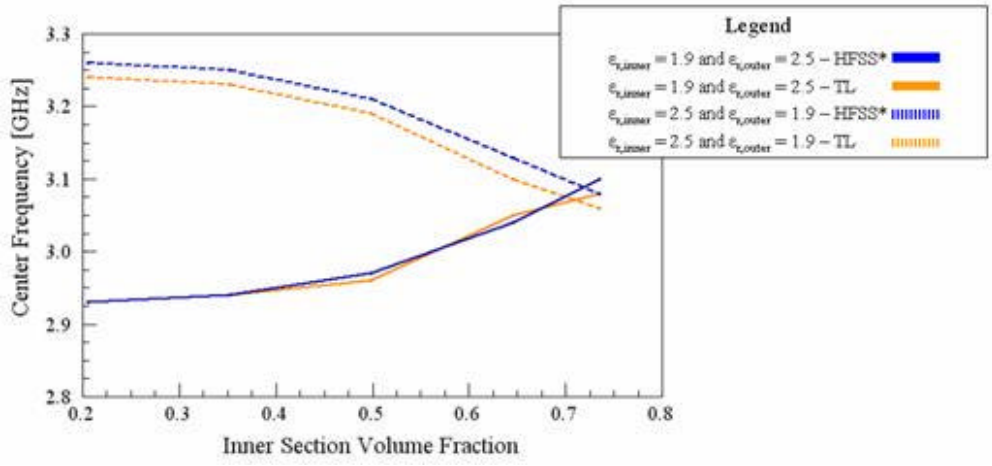

Figure 15. Center frequency versus inner section volume fraction plot for TL model results and 100 MHz shifted HFSS results.

3.0 Conclusions

The sectioned substrates investigated here were shown to give bandwidth improvements of 10% and in addition, were shown to produce maintained radiation characteristics. Effective permittivity analysis was completed and was shown to be better suited for media with more continuous properties. The secondary analysis, completed by way of transmission line modeling, was shown to give an improved characterization of the sectioned substrate patch antennas by taking the sections into account individually as opposed to averaging them.

Future Work

Future work will include an investigation of the use of more aggressive variations in the section permittivities along with smooth grading of permittivity along the sections. This work will also include the use of the transmission line model with transmission line theory to further improve the performance of the sectioned substrate designs. Fabrication and verification of these sectioned substrate antennas in our lab will be completed to complement the simulation work. Finally, we will investigate the use of our sectioned substrate techniques in unison with the loading and slot etching techniques. Joshua Fladie will continue this work to complete his master's thesis in the Spring of 2006.

References

[1] W. F. Richards and Y. T. Lo, "Theoretical and experimental investigation of a microstrip radiator with multiple lumped linear loads," *Electromagnetics*, vol. 3, no. 3-4, pp. 371-385, July-December 1983.

[2] W. F. Richards and S. A. Long, "Impedance Control of Microstrip Antennas Utilizing Reactive Loading," *Proc. Intl. Telemetering Conf.*, pp. 285-290, Las Vegas, 1986.

[3] K.L. Wong and J. Y. Wu, "Bandwidth Enhancement of Circularly-polarized Microstrip Antenna using Chip-resistor Loading," *Electron. Lett*., vol. 33, pp. 1749-1751, 1997.

[4] Z. D. Liu, P. S. Hall, and D. Wake, "Dual-frequency Planar inverted-F antenna," *IEEE Trans. Antennas Propag*., vol. 45, pp. 1451-1458, Oct. 1997.

[5] C. R. Rowell and R. D. Murch, "A Compact PIFA Suitable for Dual-frequency 900/1800-MHz Operation," *IEEE Trans. Antennas Propag.*, vol. 46, pp. 596-598, Apr. 1998.

[6] M. Yang and Y. Chen, "A Novel U-shaped Planar Microstrip Antenna for Dual-Frequency Mobile Telephone Communications," *IEEE Trans. Antennas. Propag*., vol. 49, pp. 1002-1004, June 2001.

[7] K. F. Tong, K. M. Luk, K. F. Lee, and S. M. Shum, "Analysis of broadband U-slot microstrip antenna," *IEE Tenth Int. Conf. Antennas Propag*., vol. 1, 1997, pp. 110-113.

[8] Y. L. Chow and K. H. Shiu, "A Theory on the Broadbanding of a Patch Antenna," *Asia-Pacific Microwave Conf. Proc*., vol. 1, 1997, pp. 245-248.

[9] S. Weigand, G. H. Huff, K. H. Pan, and J. T. Bernhard, "Analysis and Design of Broad-band Single-layer Rectangular U-slot Microstrip Patch Antennas," *IEEE Trans. Antennas Propag*., vol. 51, no. 3, pp. 457-468, March 2003.

[10] G. Kiziltas, D. Psychoudakis, and J. L. Volakis, "Topology Design Optimization of Dielectric Substrates for Bandwidth Improvement of Patch Antennas," *IEEE Trans. Antennas Propag*., vol. 51, no. 10, pp. 2732-2743, Oct. 2003.

[11] H. Mosallaei and K. Sarabandi, "Magneto-dielectrics in Electromagnetics: Concept and Applications," *IEEE Trans. Antennas Propag*., vol 52, no. 6, pp. 1558-1567, June 2004.

[12] Ansoft Corporation, Pittsburg, PA, *Ansoft HFSS*, Version 9.1.

[13] W. L. Stutzman and G. A. Thiele, *Antenna Theory and Design*, New York: John Wiley & Sons, Inc., 1998, pp. 225.

[14] E. O. Hammerstad, "Equations for Microstrip Circuit Design," *Proc. Fifth European Microwave Conf.*, pp. 268-272, September 1975.

[15] A. G. Derneryd, "A Theoretical Investigation of the Rectangular Microstrip Antenna Element," *IEEE Trans. Antennas Propag.*, vol. AP-26, no. 4, pp. 532-535, July 1978.

[16] I. J. Bahl and D. K. Trivedi, "A Designer's Guide to Microstrip Lines," *Microwaves*, May 1977, pp. 174-182.

[17] R. F. Harrington, *Time-Harmonic Electromagnetic Fields*, New York: McGraw-Hill Book Co., 1961, p. 183.

[18] J. S. Wright, W. J. Chudobiak, and V. Makios, "Equivalent Circuits of Microstrip Impedance Discontinuities and Launchers," *IEEE Trans. Microwave Theory Tech.*, pp. 48-52, Jan. 1974.

Publications Resulting from this Work

J. Fladie and J. T. Bernhard, "Analysis of sectioned substrate patch antennas utilizing a deterministic approach," *Proc. 2005 IEEE/URSI International Symposium on Antennas and Propagation*, July 2005.

J. Fladie and J. T. Bernhard, "Sectioned substrate microstrip patch antennas: bandwidth enhancement and modeling," Journal paper in preparation.